

Heterogeneous & Homogeneous & Bio- & Nano-

CHEM **CAT** CHEM

CATALYSIS

Accepted Article

Title: C-H Activation of Methane to Formaldehyde on Ce_{1-x}Zr_xO₂ Thin films : A step to bridge the material gap

Authors: Anjani Dubey, SAdhu Kolekar, and Chinnakonda Subramanian Gopinath

This manuscript has been accepted after peer review and appears as an Accepted Article online prior to editing, proofing, and formal publication of the final Version of Record (VoR). This work is currently citable by using the Digital Object Identifier (DOI) given below. The VoR will be published online in Early View as soon as possible and may be different to this Accepted Article as a result of editing. Readers should obtain the VoR from the journal website shown below when it is published to ensure accuracy of information. The authors are responsible for the content of this Accepted Article.

To be cited as: *ChemCatChem* 10.1002/cctc.201600670

Link to VoR: <http://dx.doi.org/10.1002/cctc.201600670>

WILEY-VCH

www.chemcatchem.org

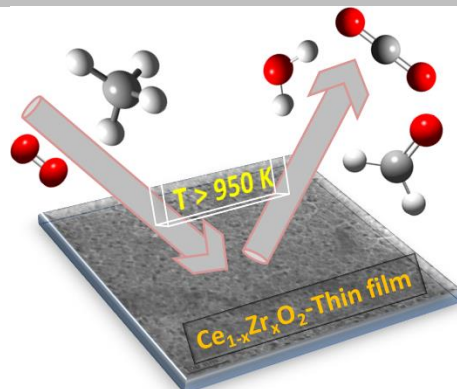


Entry for the Table of Contents

FULL PAPER

Kiss me momentarily and often

C-H activation of CH₄ to HCHO was explored under technically relevant conditions on porous Ce_{1-x}Zr_xO₂ thin films with an aim to address the material gap and mechanistic aspects. Migration of electron rich oxygen vacancy sites to the surface is responsible for HCHO formation. Low contact time and fast excursion between CH₄ and O₂ rich compositions could improve the HCHO selectivity further.



*Anjani Dubey, Sadhu K. Kolekar, and Chinnakonda S. Gopinath**

Page No. – Page No.

C-H Activation of Methane to Formaldehyde on Ce_{1-x}Zr_xO₂ Thin films : A step to bridge the material gap

Accepted Manuscript

C-H Activation of Methane to Formaldehyde on $\text{Ce}_{1-x}\text{Zr}_x\text{O}_2$ Thin films : A step to bridge the material gap

Anjani Dubey,^[a] Sadhu K. Kolekar^[a] and Chinnakonda S. Gopinath^{[a,b]*}

^[a]Catalysis Division, National Chemical Laboratory, Dr.Homi Bhabha Road, Pune 411 008, India

^[b]Center of Excellence on Surface Science, National Chemical Laboratory, Dr.Homi Bhabha Road, Pune 411 008, India.

Email: cs.gopinath@ncl.res.in; Ph: 91-20-2590 2043; <http://academic.ncl.res.in/csgopinath>

Abstract: $\text{Ce}_{1-x}\text{Zr}_x\text{O}_2$ (ceria-zirconia - CZ) thin films were prepared by a combination of sol-gel and spin coating method and evaluated for C-H activation of methane in a molecular beam setup towards bridging the material gap. C-H activation of methane begins at 950 K, and Ce-rich CZ composition displays high selectivity (4-12 %) to partially oxidized product, formaldehyde. 10-12 % selectivity towards HCHO with 1.6 % methane conversion was observed with methane-rich $\text{CH}_4:\text{O}_2$ reactants compositions at 1050 K. Low contact time conditions, prevalent under molecular beam experimental conditions, could be a possible reason for HCHO formation. While combustion products were observed instantly upon shining reactants mixture on CZ surfaces, up to 20 s delay was observed to begin formaldehyde generation underscoring the oxygen vacancy migration predominantly contributes to the rate determining step and diffusion controlled nature. A burst in HCHO generation at the point of molecular beam open, after every beam close conditions, underscores the diffusion of oxygen vacancies to the surface which is the reason for HCHO formation. Kinetic results also indicate the necessity of reduction sites for HCHO generation.

Keywords: *Heterogeneous catalysis, contact time, diffusion control, C-H activation, material gap.*

1. Introduction:

Selective conversion of methane to oxygenates, such as formaldehyde, is important to exploit natural gas reserves. Formaldehyde is the simplest aldehyde which is an important precursor for many useful chemical compounds. The direct and selective oxidation of methane to oxygenates is very difficult process as it requires high temperature (~1000 K and above) for the activation of C-H bond.^[1] In the past few decades many efforts have been made to prepare active catalysts for methane to oxygenates with molecular oxygen.^[2] Despite the serious efforts, low yield and selectivity was observed.^[3] Direct oxidation of methane to formaldehyde is possibly more efficient due to heat integration, and certainly a simpler method than steam reforming of methane to syngas process, which is the initial step for production of formaldehyde.^[4] Activation of C-H bond occurs on ceria-zirconia (CZ) catalyst with an activation energy of 439 kJ/mol. HCHO selectivity is very low as it is thermodynamically unstable and it further oxidizes to CO₂ at high temperatures, (Eqns. 1 and 2), which leads to low selectivity.^[5,6]



One of the main problems is the high contact time prevalent in the fixed bed reactors being widely employed for methane oxidation. It is generally around 1 s for methane oxidation in fixed bed reactors.^[1-2] Probably the best activity reported so far is with monomeric or isolated vanadium supported on mesoporous silica by Nguyen et al^[7] at very high GHSV (80000 to 740000 L/kg_{cat} h) or low contact time with methane conversion up to 6 % and HCHO selectivity between 57-93 %. It is also well known that changes in contact time influence the selectivity to a large extent.^[8-11] Molecular beam offers the single collision condition of reactants on catalyst surfaces and hence offers to decrease the contact time by few orders of magnitude.

Methane partial oxidation to formaldehyde with high selectivity at low methane conversion has been reported with MoO₃, V₂O₅, Nb₂O₅.^[7-11] Michalkiewicz et al.^[9] employed polymorphic niobium (V) oxides (H-Nb₂O₅ and M-Nb₂O₅) as a catalyst and evaluated methane conversion to formaldehyde between 693 and 1023 K; 78 % formaldehyde selectivity was observed at 0.2 % methane conversion at a contact time of 0.9 s and 1000 K. More than 0.2 % methane conversion decreases the selectivity exponentially. Nedyalkova et al.^[11] synthesized Fe-doped CZ fluorite catalyst and found that low temperature partial oxidation of methane to formaldehyde occurs between 573 and 873 K; while HCHO selectivity was observed to be 20 to

55 % below 673 K, methane conversion is less than 0.5 %. When methane conversion increases to 6 % at ≥ 773 K HCHO selectivity decreases to 2-4. Banares et. al.^[12] carried out partial oxidation of methane on silica supported transition metal (V, Mo, W and Re) oxide and found that 0.8 wt % MoO_x/SiO₂ shows the maximum activity with 13.9 % methane conversion. Highly monodispersed vanadium oxide^[13] and molybdenum oxide^[14] on high surface area support shows the better activity for methane oxidation to formaldehyde. Zhang et. al.^[15] claimed that NO₂ promotes the partial oxidation of methane and lowers the reaction temperature by 300 K (from 1173 to 873 K). They also claim that NO₂ favours the formation of oxidation product at the expense of C₂ hydrocarbon. Weng et. al.^[16] has carried out partial oxidation of methane to formaldehyde on Mo/Sn/P silica supported catalyst in temperature regime of 848 to 948 K. They achieved 2 to 5.8 % methane conversion with 91.9 to 30.6 % HCHO selectivity; selectivity decreases with an increase in reaction temperature. Indeed, above discussion underscores the complexity of the problem; however, low CH₄ conversion generally favours HCHO formation.

We investigated C-H activation of methane to HCHO on Ce_{1-x}Zr_xO₂ (CZ; x = 0.1 to 1) thin films in a home-built molecular beam (MB) instrument (MBI).^[17] Zr-introduction into the ceria lattice improves the redox properties of CZ along with thermal stability, which prevents agglomeration at high temperatures.^[18-19] Brinker et al and Niemantsverdriet et al used different methods to prepare thin films, with the aim to bridge the material gap.^[20,21] Our earlier report on porous CZ thin films addresses bridging the material and pressure gaps by correlating the oxygen storage capacity (OSC) measured in MBI and CO oxidation activity measured on powder CZ catalysts at ambient pressure.^[22a] One to one correlation was observed between the above two extreme conditions makes the method relevant to address material gap problems. Mn-doped CZ films have been employed for methane to syngas conversion.^[22b] From the present MBI study on CZ films, it has been observed that high cerium content of CZ film increases partial oxidation activity. C-H activation of methane to HCHO on Ce-rich CZ thin film starts at ≥ 950 K and Ce_{0.9}Zr_{0.1}O₂ shows partial oxidation of CH₄ to HCHO at T ≥ 1000 K and its activity increases with increase in temperature. Present article is focussed on bridging the material gap and related aspects, rather than finding a new or improved catalyst for methane activation. Further, emphasis is given to understand the reaction mechanism aspects through molecular beam approach.

2. Experimental section

CZ ($\text{Ce}_{1-x}\text{Zr}_x\text{O}_2$) thin films were prepared by a combination of sol-gel and spin coating method on Si wafer (MaTeck Germany, 99.9 % pure).^[22-23] General characterisation about the films by x-ray diffraction (XRD), Raman spectroscopy, surface profilometer, transmission electron microscopy (TEM) are given in the supporting information (see SI-1) along with preparation details. The custom built ambient pressure photoelectron spectrometer (Prevac, Poland) equipped with VG Scienta R3000HP analyzer and monochromatic Al K α x-ray (1486.6eV) was used to record the core levels of different elements of CZ thin films.^[24]

C-H activation experiments was performed in a 22 L capacity home-built MBI.^[17,25] Base pressure of the chamber was maintained in typical ultra high vacuum (UHV) around 2×10^{-10} Torr. MBI was equipped with a quadruple mass spectrometer (Pfeiffer, HiQuadTM, QMG 700 with QMA 410, 1-128 amu) to observe the change in partial pressure of reactants and products. Molecular beam (MB) can be closed or open at will with the help of a shutter placed between the MB doser and thin film. Elaborate details about MB generation and various parameter calculations are available in ref. 25. CZ film spun coated on Si wafer has been placed in niobium sample holder which can be resistively heated unto 1150 and cooled unto 125 K with liquid nitrogen. Cr-Al (K-type) thermocouple was spot welded on the sample holder to measure temperature of the assembly containing sample as well as sample holder. Selective oxidation of methane to HCHO has been measured on CZ thin film under isothermal conditions at different reaction temperatures. Between any two successive measurements, surface was regenerated by simple oxygen treatment at 773 K for 20 min.

3.0 Results and Discussion:

3.1 Textural and Spectral Characteristics of $\text{Ce}_{1-x}\text{Zr}_x\text{O}_2$ thin film:

X-ray diffraction results are shown in Fig. SI-2. CZ thin film on Si wafer is crystalline in nature and from the diffraction pattern it was identified that the structure to be cubic fluorite and as that of ceria. Surface profile and thickness of the film was measured by surface profilometer at different positions. Thickness was observed to be in the nano-regime between 30 and 50 nm, which is homogeneous and uniform from small to large area (Fig. 1). Surface profiles also show some sporadic spikes, which is due to Si substrate and not from thin film.^[22] Surface profile measured separately on Si-substrate supports this. It has been found from surface profile analysis that as the Ce content of CZ film increases porosity of CZ thin film also increases. In fact, thickness and surface roughness appears to be similar (40 nm) for $\text{Ce}_{0.9}\text{Zr}_{0.1}\text{O}_2$ composition.

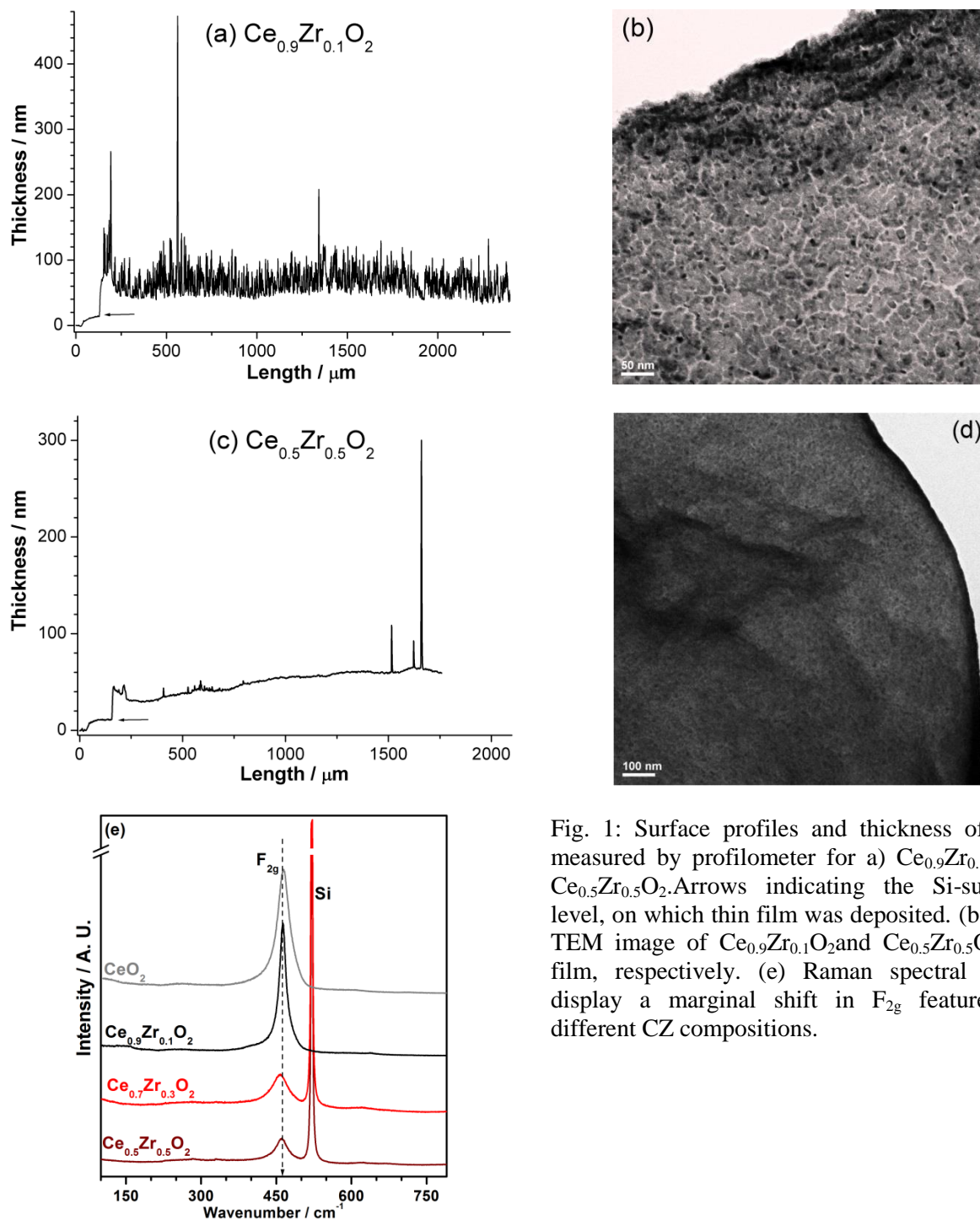


Fig. 1: Surface profiles and thickness of films measured by profilometer for a) $\text{Ce}_{0.9}\text{Zr}_{0.1}\text{O}_2$, c) $\text{Ce}_{0.5}\text{Zr}_{0.5}\text{O}_2$. Arrows indicating the Si-substrate level, on which thin film was deposited. (b and d) TEM image of $\text{Ce}_{0.9}\text{Zr}_{0.1}\text{O}_2$ and $\text{Ce}_{0.5}\text{Zr}_{0.5}\text{O}_2$ thin film, respectively. (e) Raman spectral results display a marginal shift in F_{2g} feature with different CZ compositions.

TEM analysis also indicates the CZ films synthesized are porous in nature, which is also shown in Fig. 1.^[22,23] Porous nature of the film brings in the characteristic of real world catalyst, which helps for diffusion of reactants and products.

CeO₂ catalyst exhibits a strong characteristic peak at 464 cm⁻¹, which correspond to the F_{2g} vibration mode of cubic fluorite structure (Fig. 1e). This feature arises due to the symmetric arrangement of O-atoms in the cubic fluorite structure with Fm3m space group. However, upon introduction of 10 atom % Zr in ceria, a marginal peak shift was observed and narrow peak appears at 461 cm⁻¹; while it appears at 457 cm⁻¹ and 460 cm⁻¹ for 30 and 50 atom % Zr⁴⁺ ions into ceria lattice, respectively. It was also observed that with increase in Zr⁴⁺ content there is a linear decrease in intensity of F_{2g} peak was observed. This is mainly due to the symmetry breaking in the ceria lattice due to the formation of CZ solid solution. Since Zr⁴⁺ ionic radii (84 pm) is lower than that of Ce⁴⁺ (94 pm), to minimize the structural stress larger size Ce³⁺ and some oxygen vacancy (O_v) occurs; this leads to a lattice contraction (Fig. SI-2) which causes a red shift in Raman results. No sign of ZrO₂ feature was observed in Raman results suggesting the solid solution nature of CZ. Sharp feature observed at 520 cm⁻¹ is due to Si-substrate.

XPS measurements were made on CZ thin films and Fig. 2a shows the Ce 3d core level spectra, which is complex in nature. Two sets of multiplets were observed which is symbolized as v and u for 3d_{5/2} and 3d_{3/2} spin-orbit doublets. A total of ten features appear due to various final states and extensive literature reports are available.^[26] Two prominent features of Ce³⁺, which appears at 884.6 eV (v^ˆ) and 903.2 eV (u^ˆ) (indicated by dashed arrows), increases in intensity and suggesting an increasing Ce³⁺ content with increasing Zr-content.^[26] Fig. 2b shows the Zr 3dspectra of CZ thin film which shows two peaks at 182.9 and 185.3 eV, corresponds to 3d_{5/2} and 3d_{3/2} spin-orbit doublets.^[27] As the Ce content of CZ film increases there is a minor shift observed towards higher BE in Zr 3d spectra; indeed this indicates a change in electronic environment of CZ surfaces upon Zr-introduction into the ceria lattice. Fig 2c shows O 1s spectra of CZ thin film. The feature observed at 530.3 eV (532.6 eV) corresponds to lattice (hydroxyl) oxygen of CZ surfaces. A careful look at the spectra reveals a narrowing of the valley between the above two features with increasing Ce-content, suggesting the presence of third component. This is attributed to those O-atoms that are closer to O_v sites. Introduction of Zr into ceria lattice changes the stoichiometry of Ce^{4+/3+}, which is responsible for O_v content.^[28]

3.2 Molecular Beam Studies of Methane oxidation on Ce_{0.9}Zr_{0.1}O₂ thin film.

MB measurements were made for oxygen adsorption for three CZ compositions and the results are shown in Fig. SI-3.^[22] Generally, the rate of O₂ adsorption increases with increase in temperature for any CZ composition. Cerium-rich CZ film (Ce_{0.9}Zr_{0.1}O₂) has shown high rate

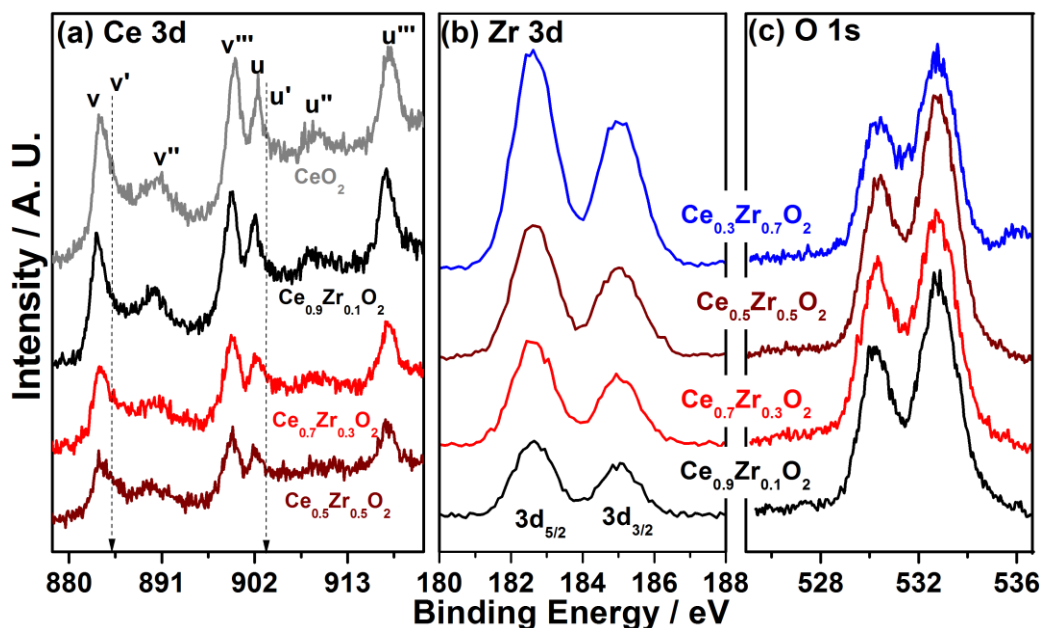


Fig. 2 XPS spectra of a) Ce 3d, b) Zr 3d and (c) O 1s core levels of $\text{Ce}_{1-x}\text{Zr}_x\text{O}_2$ thin film.

of oxygen adsorption and also high oxygen storage capacity (OSC). Detailed studies of oxygen adsorption on CZ thin films have been reported in our earlier publication and readers are requested to refer ref. 22. Partial oxidation of methane on CZ thin films have been measured and it is found that Ce-rich thin film exhibits high activity and in correspondence with oxygen adsorption characteristics. Partial oxidation of methane along with kinetic parameters have been studied and discussed in detail, particularly for $\text{Ce}_{0.9}\text{Zr}_{0.1}\text{O}_2$ composition.

Fig. 3 shows the first sign of methane oxidation at 950 K with $\text{CH}_4:\text{O}_2 = 1:2$ ratio on $\text{Ce}_{0.9}\text{Zr}_{0.1}\text{O}_2$ thin film; however, the same was not observed at 950 K with methane rich compositions, such as $\text{CH}_4:\text{O}_2 = 1:1$ (see SI, Fig. SI-4). At 950 K, only combustion products were observed with stoichiometric and more oxygen containing $\text{CH}_4 + \text{O}_2$ mixture. Although oxygen adsorption was observed below 950 K, no methane oxidation/activation was observed with any CZ compositions. At $t = 25$ s molecular beam of reactants mixture was allowed into the UHV chamber with shutter in closed position; this prevents direct interaction of MB with the surface of catalyst. Partial pressure of methane and oxygen increases immediately. At $t = 45$ s shutter was opened which allows direct adsorption of reactants on the surface of the catalyst. O_2 adsorption was observed immediately on shutter opening with sign of marked decrease in partial pressure, which indicates the consumption of O_2 during the course of reaction. No fast changes in partial pressure for methane, unlike in the case of O_2 , was observed for shutter oscillation; this

is mainly due to very small sticking coefficient of CH_4 .^[29,30] However, a gradual and noticeable change observed for adsorption of methane on shutter opening. Difference in partial pressures between shutter open and close positions has been used for methane conversion calculations. A gradual increase in partial pressure of H_2O and CO_2 was observed along with oxygen and methane adsorption. CO_2 (H_2O) reaches the steady state at $t = 155$ s (105 s). Thus we observe relatively slow CO_2 formation kinetics, which directly indicates that reaction proceeds via diffusion controlled process due to porous nature of CZ thin films. Being the smallest in size and mass, H-atoms diffuse fast into the pores and reacts with lattice oxygen to form water molecules.

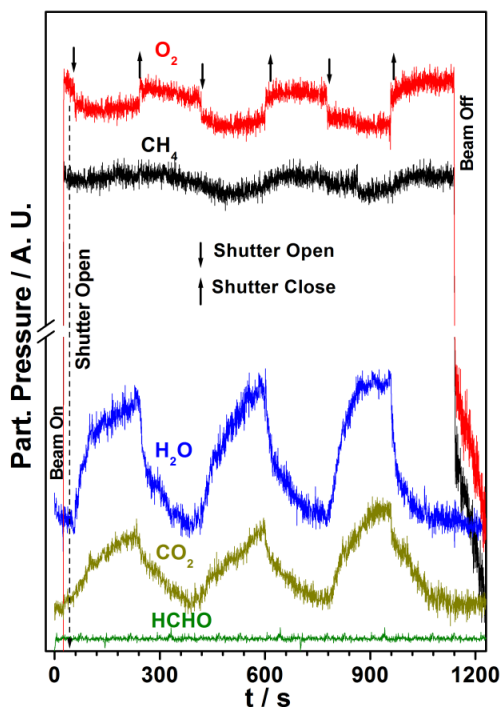


Fig. 3: Experimental kinetic data for oxidation of CH_4 with O_2 in 1:2 ratio at 950 K on $\text{Ce}_{0.9}\text{Zr}_{0.1}\text{O}_2$ thin film. Molecular beam oscillation was made for every 180 s. Only combustion products were observed. Up and down arrow signs for shutter closing and opening, respectively, are used in all figures.

At $t = 240$ s shutter was closed which prevents direct interaction of reactants on the catalyst; however this leads to a decrease in partial pressure of CO_2 and H_2O and it reaches the background level at $t = 330$ s. Similarly, reactants partial pressure reaches the original level observed before shutter opening at the first instance. No other partially oxidized products were observed, including HCHO. The oscillation of the molecular beam has been made several times to reproduce the kinetic data. Further several parameters, like variation of reaction temperature,

O₂-rich to CH₄-rich compositions has been studied and described below. All the reactions reported in this communication have been reproduced at least three times on the same CZ compositions within an error margin of 10 %. In fact this hints the quality of surface and thin film remains the same.

Fig. 4 shows the experimental kinetic data for the oxidation of methane with CH₄:O₂ = 1:1 composition at 1000 K on (a) Ce_{0.9}Zr_{0.1}O₂, as well as (b) Ce_{0.7}Zr_{0.3}O₂ compositions. On opening the shutter at t = 55 s (dashed line, Fig. 4a), CO₂ and H₂O forms, which is similar to the results discussed in Fig. 3. However, both H₂O and CO₂ reach the steady state at t = 200 and 125 s, respectively; this observation is similar to the combustion products evolution at 950 K, however with relatively fast kinetics. Indeed, partial pressure of water initially overshoots the steady state level indicating a fast diffusion of H-atoms to form water molecules at high temperatures. Along with combustion products, interestingly, HCHO formation begins, albeit, after a delay of 20 s at t = 75s. In fact, a sudden burst in HCHO was observed at the time of shutter opening (t = 55 s), and the same subsides immediately. Spike in HCHO partial pressure was reproducibly observed at the point of opening shutter and one such example is shown in the inset of Fig. 4a. HCHO production reaches the steady state at t = 153 s, which is longer than that for combustion products. This underscores the slow formation kinetics of HCHO and predominantly contributes to the rate determining step for the overall reaction. In general, rate of reaction increases with increase in reaction temperature, which can be easily identified by an increase in consumption of O₂, as well as larger amount of products formation, compared to the reaction at 950 K. Selectivity and yield of HCHO is less compared to CO₂, as the heat of combustion of HCHO is highly exothermic than methane (Equ. 1 and 2).^[6] While closing the shutter at t = 240 s the partial pressure of all product i.e. CO₂, H₂O and HCHO decreases and it attains the background level. CO₂ takes only 10 s to reach the new steady state at t = 250 s, while H₂O and HCHO takes 65 s to reach steady state indicating that the delay in attaining the new steady state for HCHO is probably due to its further oxidation into CO₂ and H₂O.

MB oscillation was made at least three times to ensure the kinetic data is reproducible within the experimental error limit of 10 %. Every time the shutter was opened, importantly, sudden burst in HCHO partial pressure was observed followed by HCHO production after about 20 s delay. We attribute this observation to the following: It is very likely that HCHO formation requires catalytic sites that are rich with electrons, such as Ce³⁺ and associated O_v sites. Fully

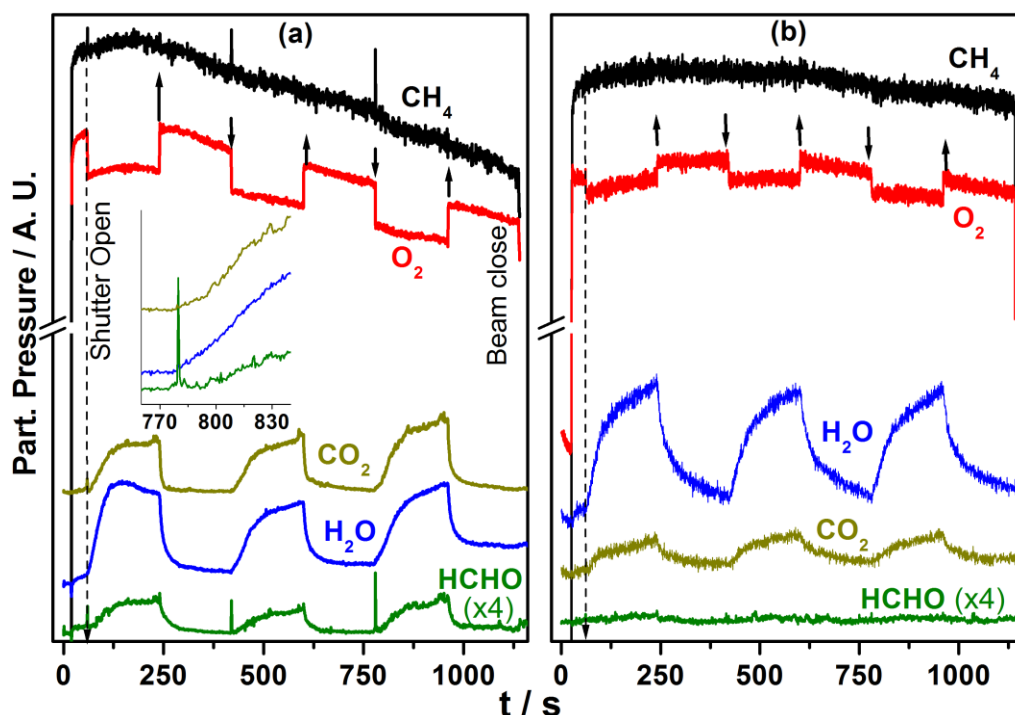


Fig. 4. Experimental kinetic data for selective oxidation of CH_4 with O_2 in 1:1 ratio on a) $\text{Ce}_{0.9}\text{Zr}_{0.1}\text{O}_2$ and b) $\text{Ce}_{0.7}\text{Zr}_{0.3}\text{O}_2$ thin film at temperature $T = 1000$ K. The shutter operation i.e. opening and closing of MB was made after every 180 s.

oxidized sites would lead to total oxidation products. After closing the shutter, due to the unavailability of reactants directly, as well as due to high temperatures, CZ surface is likely to be enriched with O_v and Ce^{3+} . This factor induces a sudden spurt in HCHO on opening the shutter. Three points are worth highlighting about this observation. First is the direct conversion of methane to HCHO, albeit in a short burst. Second is the availability of plenty of oxygen from the direct beam of reactants makes the surface more oxidizing and hence combustion products formation increases instantly. Oxygen diffusion into the subsurface and bulk brings in the O_v to the surface and HCHO formation picks up gradually after a delay time of 20 s at 1000 K, and reaches the steady state again. Third point to be noted is an increase in CO_2 and H_2O background level pressure, while HCHO remains at the initial level, under beam off conditions after MB oscillations, indicating the diffusion nature of the entire reaction. Fig. 4b shows the oxidation of methane to combustion products at 1000 K on $\text{Ce}_{0.7}\text{Zr}_{0.3}\text{O}_2$ composition, with no marginal sign of HCHO formation. Similar results were observed for other Zr-rich CZ composition thin films.

Fig. 5a shows the experimental data for oxygen adsorption during the course of reaction at 1000 K with various $\text{CH}_4:\text{O}_2$ ratio from 5:1 to 1:5. Figs. 3, 4 and 5a emphasize that oxygen

was consumed predominantly under reaction conditions and irrespective of reactants composition; this leads to an inevitable formation of the combustion products, especially with O₂-rich reaction mixture. Fig. 5b shows the rate of oxygen adsorption with various O₂/CH₄ ratios at 1000 and 1050 K. Although oxygen adsorption increases with oxygen content, careful analysis of Fig. 5b reveals a change in slope from methane-rich to oxygen-rich compositions. Rate of oxygen adsorption is relatively small with CH₄-rich compositions underscoring the hindrance for oxygen adsorption; while it is the opposite trend with O₂-rich compositions. Similar analysis show methane conversion gradually changes from 0.9 (0.08 ML/s) to 1.6 % (0.15 ML/s) from CH₄-rich (O₂:CH₄ = 1:5) to O₂-rich (O₂:CH₄ = 5:1) compositions, respectively, on Ce_{0.9}Zr_{0.1}O₂. Very likely, carbon or carbonaceous species on the catalyst surfaces due to methane-rich compositions slow down the diffusion of oxygen atoms into the sub-surface and bulk; this is in addition to the oxygen consumption for CO₂ and H₂O formation.

Fig. 6 shows the dependence of products evolution as a function of time and O₂:CH₄ ratio at 1000 K. Evolution of all products was plotted in separate panels to minimize the complexity of the reaction. Partial oxidation of methane has also been evaluated at 1050 K (results not shown), and the same trend has been found as that of at 1000 K. Irrespective of reactants composition, all products formation occurs, and the same increases form methane-rich to O₂ rich compositions. Especially, with oxygen-rich compositions above 1:1 of O₂:CH₄, the rate of products formation seems to enhance linearly. Rate of CO₂ and HCHO production shows less dependence on CH₄:O₂ ratio for methane-rich compositions. Another important point to be noted is the decrease in delay time between shutter opening and HCHO formation with oxygen rich reactants. In contrast to the expectations of total combustion with O₂-rich compositions, HCHO production at high rate indicates the active nature of the surface. With more oxygen supply at high temperatures, the oxygen diffusion to the bulk is also expected to be faster and this in turn enhances the O_v diffusion to the surface, which favours high rate of HCHO formation. More carbon species (C, CH_x) deposition on the surface might prevent or decelerate O_v diffusion towards the surface and hence low rate of HCHO occurs with methane-rich compositions; nonetheless, CH_x species on the surface makes it significantly reduced, especially with small amount of O₂ available in gas-phase. Partial (and total) oxidation of CH₄ is facile in O₂-rich beam at high temperature, which accelerates the migration of O_v towards the surface and hence the rate increases.^[31]

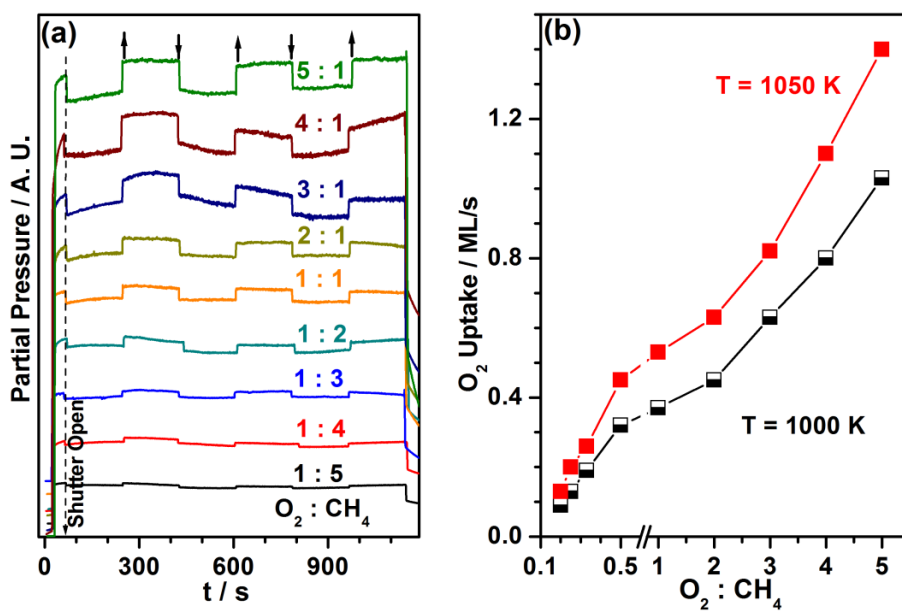


Fig. 5. a) Experimental data for O₂ adsorption, and b) rate of oxygen adsorption during the course of reaction with different O₂/CH₄ ratio at T = 1000 and 1050 K on Ce_{0.9}Zr_{0.1}O₂.

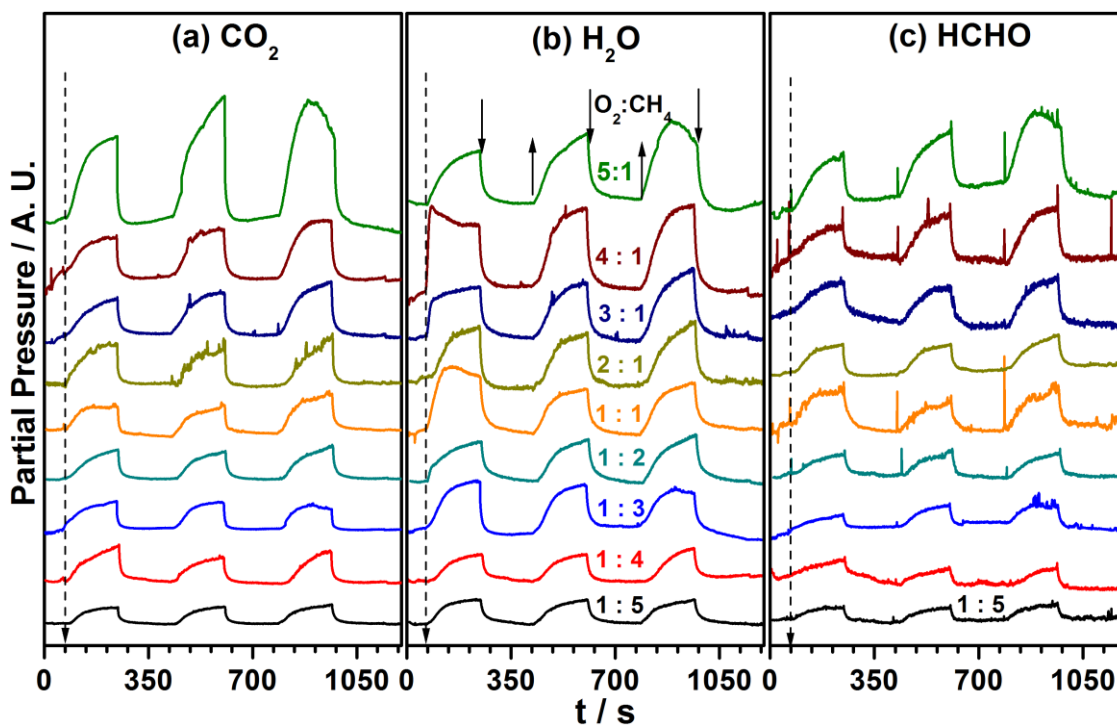


Fig. 6. Products evolution as a function of time at 1000 K for different O₂:CH₄ ratios for a) CO₂, b) H₂O, and c) HCHO.

Rate of formation of formaldehyde and combustion products has been calculated from Fig. 6 under steady state conditions. Fig. 7 shows the rate of formation of products, (a) CO₂, (b)

H₂O, and (c) HCHO, as a function of O₂/CH₄ ratio, at 1000 and 1050 K. Percent ratio of rate of formation of HCHO to HCHO + CO₂, which is selectivity of HCHO among carbon containing products, is plotted in Fig. 7d. It has been found from Fig. 7 that the rate of formation of products increases with increase in O₂/CH₄ ratio. There is a slow and steady increase upto O₂/CH₄ ratio of 2. A breakthrough in the overall rate is observed at a ratio of 3. Rate of formation of all products increased 3-5 times that of methane rich composition. This trend is highly prominent at 1050 K. Rate increase observed for all products underscores an enhancement in methane conversion also to a similar extent. Percent selectivity of HCHO is an important factor, which is shown in Fig. 7d. Not surprisingly, selectivity is found to be higher for the methane rich beam and it is found to

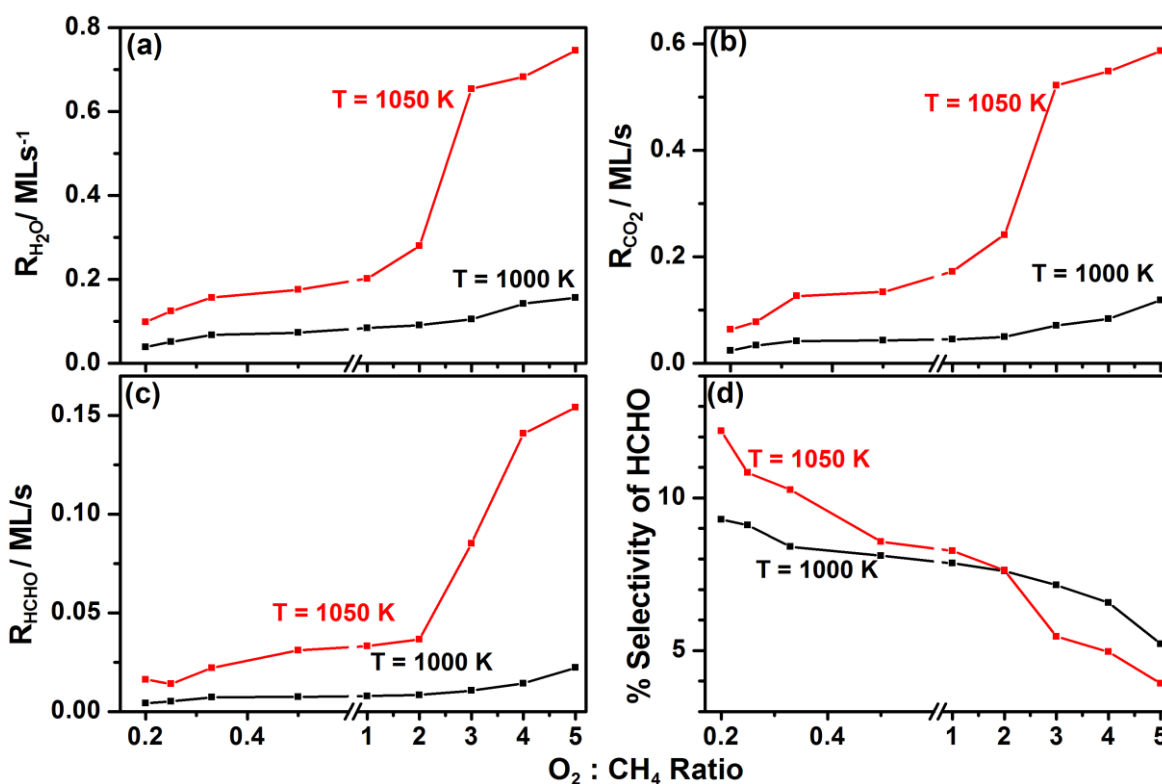


Fig. 7 Rate of formation of oxidation products, a) H₂O, b) CO₂, c) HCHO and d) HCHO/CO₂ ratio at two different temperatures as a function of O₂/CH₄ ratio.

be the highest at 12.2 % for 5:1 ratio of CH₄:O₂ at 1050 K. With an increase in O₂ content, selectivity towards HCHO decreases. It was also found that with increase in temperature HCHO selectivity increases up to O₂/CH₄ ratio of 2, thereafter selectivity decreases with increase in O₂ rich compositions. Nevertheless, 12.2 % selectivity observed is better or comparable to the

values reported for many of the reported catalyst systems.^[8-9] However, compared to the vanadia-based catalyst,^[7,13] activity is lower with present CZ catalyst. Lin et al^[32] observed HCHO selectivity of 90 % at 873 K using MoO₃/SiO₂ catalyst with low CH₄ conversion but as the temperature increases to 983 K selectivity becomes zero; compared to this Ce_{0.9}Zr_{0.1}O₂ thin film shows a maximum selectivity of 12.2 %. However, considering the significantly large activity in a burst of few seconds in the transient state (Fig. 4a inset, and Fig. 6c) followed by a relatively slow HCHO kinetics, activity enhancement can be further manipulated by quick oscillations between oxygen-rich and oxygen-lean reactant compositions. Oxygen-lean composition, due to its reduction nature, is expected to migrate fast and more O_v to the surface, while allowing methane adsorption leading to more HCHO. This would allow the HCHO generation selectivity, at least, to double (20-25 %) by carefully maintaining the transient bursts. However, more careful experiments are necessary to confirm this hypothesis.

It is also surprising that carbon monoxide was not observed in any of our experiment, although it is very much expected. Possible reason could be its further oxidation to CO₂ due to porous nature of CZ. 100 % CO oxidation to CO₂ was observed on Ce_{0.9}Zr_{0.1}O₂ above 625 K.^[22a] To the best of our knowledge, complex reactions, such as methane activation has not been measured on thin films of real-world catalysts in surface science setup such as MBI. Present work underscores the direct conversion of methane to formaldehyde on reduced Ce³⁺ and oxygen vacancy sites.

Conclusion. Partial oxidation of methane has been carried out on various compositions of ceria-zirconia solid solution thin films in a home-built molecular beam setup. C-H activation of methane generally takes place at temperatures higher than 950 K. Ceria rich thin film Ce_{0.9}Zr_{0.1}O₂ exhibits partial oxidation of methane to formaldehyde at 12 % selectivity and 1.6 % methane conversion. Though rate of formation of formaldehyde increases with increase in oxygen rich reactants compositions as well as at high temperatures, HCHO selectivity remains at 12 %. No formaldehyde formation was observed with Zr-rich CZ compositions. A careful analysis of the results obtained suggests the reduction sites, such as oxygen vacancies, CH_x, are necessary for partially oxidized product. Beam oscillations carried out in the present set of experiments also indicates the necessity to quickly alter the reactants composition between methane-rich to oxygen-rich streams to maximize and manage the activity and selectivity. If large amount of oxygen adsorption can be manipulated by quick excursion between O₂-rich and

CH₄-rich compositions, more partially oxidized product can be produced and more work is suggested in this direction. Although diffusion is an integral part of catalysis phenomenon, such material gap reduction attempts allow us to explore more on this. More work from around the globe on similar lines will eventually lead to a better kinetic model for complicated reactions, such as C-H activation of methane.

Supporting Information (SI) available: Ceria-zirconia thin films synthesis and characterization (SI-1), X-ray diffraction (SI-2), oxygen adsorption on CZ thin films (SI-3), and methane oxidation on Ce_{0.7}Zr_{0.3}O₂ thin film at 950 K (SI-4) are available.

Acknowledgements

A.D. is thankful to the UGC, New Delhi for senior research fellowship. We thank BRNS (2011/37C/36/BRNS) and SERB (SR/S1/PC-16/2012) for funding this research project.

References:

1. a) H. D. Gesser, N. R. Hunter, *Chem. Rev.* **1985**, *85*, 235-244. b) J. H. Lunsford, *Catal. Today* **2000**, *63*, 165-174. c) B. C. Enger, R. Lodeng, A. Holmen, *Appl. Catal. A: Gen.* **2008**, *346*, 1-27.
2. a) C. F. Cullis, D. E. Keene, D. L. Trimm, *J. Catal.* **1970**, *19*, 378-385. b) L. C. Kao, A. C. Hutson, A. Sen, *J. Am. Chem. Soc.* **1991**, *113*, 700-701. c) S. Y. Chen, D. Willcox, *Ind. Eng. Chem. Res.* **1994**, *33*, 832-839. d) Y. Wang, K. J. Otsuka, *J. Catal.* **1995**, *155*, 256-267.
3. a) X. Yang, K. D. Jung, S. H. Cho, O. Shim, S. J. Uhm, S. H. Han, *Catal. Lett.* **2000**, *64*, 185-190. b) B. Michalkiewicz, *Appl. Catal. A: Gen.* **2004**, *277*, 147-153.
4. a) R. A. Periana, D. J. Taube, E. R. Evitt, D. G. Loffler, P. R. Wentrcek, G. Voss, T. Masuda, *Science* **1993**, *259* 340-343. b) M. Muehlhofer, T. Strassner, W. A. Herrmann, *Angew. Chem. Int. Ed.* **2002**, *41*, 1745-1747.
5. M. J. Brown, N. D. Parkyns, *Catal. Today*, **1991**, *8*, 305-335.
6. a) X. L. Sang, K. Z. Li, H. Wang, Y. G. Wei, *Rare Met.* **2014**, *33*, 230-238. b) S. B. Dworkin, A. M. Schaffer, B. C. Connelly, M. B. Long, M. D. Smooke, M. A. Puccio, B. M. Andrew, J. H. Miller, *Proc. Combustion Institutes* **2009**, *32*, 1311-1318.
7. L. D. Nguyen, S. Lorient, H. Launay, A. Pigamo, J. L. Dubois, J. M. M. Millet, *J. Catal.* **2006**, *237*, 38-48.
8. a) S. Morteza, V. Leila, *World Appl. Sci. J.* **2009**, *6*, 339-346. b) Q. Zhu, X. Zhao, Y. Deng, *J. Nat. Gas Chem.* **2004**, *13*, 191-203.
9. a) B. Michalkiewicz, J. S. Nazzal, P. Tabero, B. Grzmil, U. Narkiewicz, *Chem. Papers* **2008**, *62*, 106-113. b) F. Zaera, C. S. Gopinath, *J. Chem. Phys.* **2002**, *116*, 1128-1136.
10. M. Faraldos, M. A. Banares, J. A. Anderson, H. Hu, I. E. Wachs, J. L. G. Fierro, *J. Catal.* **1996**, *160*, 214-221.
11. R. Nedyalkova, D. Niznansky, A. C. Roger, *Catal. Commun.*, **2009**, *10*, 1875-1880.
12. M. A. Banares, L. J. Alemany, M. L. Granados, M. Faraldos, J. L. G. Fierro, *Catal. Today* **1997**, *33*, 73-83.

13. a) B. Lin, X. Wang, Q. Guo, W. Yang, Q. Zhang, Y. Wang, *Chem. Letters* **2003**, 32, 860-861. b) c) H. Berndt, A. Martin, A. Brucker, E. Schreier, D. Muller, H. Kosslick, G. U. Wold, B. Lucke, *J. Catal.* **2000**, 191, 384-400. d) A. Parmaliana, F. Frusteri, A. Mezzapica, M. S. Scurrill, N. Giordano, *J. Chem. Soc., Chem. Commun.* **1993**, 751-753.
14. a) V. A. Ebrahimi, J. J. Rooney, *J. Mol. Catal.* **1989**, 50, L17-L22. b) W. Yang, X. Wang, Q. Guo, Q. Zhang, Y. Wang, *New J. Chem.* **2003**, 27, 1301-1303.
15. J. Zhang, V. Burkle-Vitzthum, P. M. Marquaire, *Chem. Engineer. J.* **2012**, 189-190, 393-403.
16. T. Weng, E. E. Wolf, *Appl. Catal. A: General* **1993**, 96, 383-396.
17. C. S. Gopinath, A. Dubey, S. K. Kolekar, (in preparation).
18. a) E. Mamontov, T. Egami, R. Brezny, M. Koranne, S. Tyagi, *J. Phys. Chem. B* **2000**, 104, 11110-11116. b) S. Meiqing, W. Xinquan, A. Yuan, W. Duan, Z. Minwei, W. Jun, *J. Rare Earths* **2007**, 25, 48-52.
19. a) E. Aneggi, M. Boaro, C. D. Leitenburg, G. Dolcetti, A. Trovarelli, *J. Alloys & Comp.* **2006**, 408-412, 1096-1102. b) S. Damyanova, B. Pawelec, K. Arishtirova, M. V. M. Huerta, J. L. G. Fierro, *Appl. Catal. A: Gen.* **2008**, 337, 86-96. c) J. Beckers, G. Rothenberg, *Dalton Trans.* **2008**, 46, 6573-6578.
20. C. J. Brinker, G. W. Scherer, *Sol-gel Science, Academic Press, New York* **1990**, p. 180.
21. A. M. Saib, A. Borgna, J. V. D. Loosdrecht, P. J. V. Berge, J. W. Niemantsverdriet, *J. Phys. Chem. B* **2006**, 110, 8657-8664.
22. a) A. Dubey, S. K. Kolekar, E. S. Gnanakumar, K. Roy, C. P. Vinod, C. S. Gopinath, *Catal. Struct. React.* **2016**, 2, 1-12. b) A. Dubey, S.K. Kolekar, C.S. Gopinath, *ChemCatChem* **2016**, 8, 2296-2306.
23. R. Jain, A. Dubey, M. Ghosalya, C. S. Gopinath, *Catal. Sci. Technol.* **2016**, 6, 1746-1756.
24. K. Roy, C. P. Vinod, C. S. Gopinath, *J. Phys. Chem. C* **2013**, 117, 4717-4726.
25. a) K. Thirunavukkarasu, C. S. Gopinath, *Catal. Lett.* **2007**, 119, 50-58. b) K. Thirunavukkarasu, K. Thirumoorthy, J. Libuda, C. S. Gopinath, *J. Phys. Chem. B.* **2005**, 109, 13272-13282.
26. a) D. R. Mullins, *Surf. Sci. Rep.* **2015**, 70, 42-85. b) M. Engelhard, S. Azad, C. H. F. Peden, S. Thevuthasan, *Surf. Sci. Spectra* **2006**, 11, 73-81. c) B. Murugan, A. V. Ramaswamy, D. Srinivas, C. S. Gopinath, V. Ramaswamy, *Chem. Mater.* **2005**, 17, 3983-3993.
27. a) S. Velu, K. Suzuki, C. S. Gopinath, H. Yoshida, T. Hattori, *Phys. Chem. Chem. Phys.* **2002**, 4, 1990-1999. b) A. Burange, R. Shukla, A. K. Tyagi, C. S. Gopinath, *ChemistrySelect* **2016**, 1, 2673-2681.
28. a) A. Bensalem, F. Bozon-Verduarez, M. Delamer, G. Bugli, *Appl. Catal. A: Gen.* **1995**, 121, 81-93. b) E. Paparazzo, G. M. Ingo, N. Zacchetti, *J. Vac. Sci. Tech. A* **1991**, 9, 1416-1420. c) A. Pfau, K. D. Schierbaum, *Surf. Sci.* **1994**, 321, 71-80.
29. L. Jiang, H. Zhu, R. Razzaq, M. Zhu, C. Li, Z. Li, *Int. J. Hydrogen Energy* **2012**, 37, 15914-15924.
30. *CRC Handbook of Chemistry and Physics*, 85th ed.; D. R. Lide, Ed.; CRC Press: Boca Raton, FL, **2004**.
31. Q. Sun, J. M. Jehng, H. Hu, R. G. Herman, I. E. Wachs, K. Klier, *J. Catal.* **1997**, 165, 91-101.
32. Z. Lin, F. Jian, Q. F. Li, *J. Natural Gas Chem.* **1997**, 6, 322-328.